The Simulation of Irradiation Creep*

Conf-770641--6

T. C. Reiley and P. Jung†

Metals and Ceramics Division
Oak Ridge National Laboratory
Oak Ridge, Tennessee 37830

Abstract

This paper reviews the results to date in the area of radiation enhanced deformation using beams of light ions to simulate fast neutron displacement damage. A comparison is made between these results and those of in-reactor experiments. Particular attention is given to the displacement rate calculations for light ions and the electronic energy losses and their effect on the displacement cross section. Differences in the displacement processes for light ions and neutrons which may effect the irradiation creep process are discussed. The experimental constraints and potential problem areas associated with these experiments are compared to the advantages of simulation. Support experiments on the effect of thickness on thermal creep are presented. A brief description of the experiments in progress is presented for the following laboratories: HEDL, NRL, ORNL, PNL, U. of Lowell/MIT in the United States, AERE Harwell in the United Kingdom, CEN Saclay in France, GFK Karlsruhe and KFA Jülich in West Germany.

---

*Research sponsored by the Energy Research and Development Administration under contract with Union Carbide Corporation.

†On assignment from KFA Jülich, West Germany.

Introduction

Simulation of irradiation creep means creep measurements during charged particle irradiation to simulate creep processes which are induced or influenced by the neutrons in a nuclear reactor.

While damage production by charged particles, like electrons or heavy ions is already a rather common technique, the simulation of mechanical property changes has recently emerged as a promising approach to the fundamental understanding of irradiation creep processes as well as a tool for screening candidate structural materials. Actually, creep experiments under charged particle irradiation preceded the in-reactor experiments |1-3|, but as these and other early attempts |4-7| were only intended to study basic properties of creep rather than to simulate the behavior of reactor materials, they will not be discussed here in more detail.

From an experimental point of view, irradiation creep simulation poses certain constraints on the charged particles used. Light ions (p, d, ^{3}He, α) of energies between about 4 and 100 MeV are the most practical choice, and have been used in the recent experiments. Therefore, in the following we will confine our discussion to this range of energies and particles.

In this paper we discuss the general experimental procedure, the recent results and the basic similarities and differences between light ion irradiation creep and neutron irradiation creep. These are compared on the basis of the displacement processes, energy losses and experimental restrictions.

Displacement Calculations

The number of displacements per atom (dpa) is a widely used measure for comparing the exposure to different particles in simulation experiments. The displacement rate, K [dpa-sec^{-1}], divided by particle flux ϕ [particles/m^2-sec], (this ratio is also called the displacement cross section, σ_d) is derived by the following equation:

$$\frac{K}{\phi} = \sigma_d = \int_{T_d}^{T_m(E)} \frac{d\sigma_d(E,T)}{dT} \nu(T)\, dT \;, \qquad (1)$$

where $d\sigma_d/dT$ is the differential cross section which gives the probability that a lattice atom receives a recoil energy T from an irradiation particle of energy, E. For light ions $d\sigma_d/dT$ is given over a wide range by the Rutherford cross section:

$$\left(\frac{d\sigma_d}{dT}\right) \left[\frac{m^2}{ev}\right] = 6.5 \times 10^{-24} \cdot \frac{M_1}{M_2} \cdot Z_1^2 Z_2^2 \, \frac{1}{E[\mathrm{MeV}]} \cdot \frac{1}{T^2[\mathrm{eV}]} \;, \qquad (2)$$

where Z_1, Z_2, and M_1, M_2 are atomic numbers and weights of particles and target atoms, respectively. $\nu(T)$ describes the number of atoms displaced per primary recoil of energy T and is calculated according to a generally |8| accepted procedure using a modified Kinchin-Pease (KP) |9| model:

$$\nu_{KP}(T) = \frac{0.8(T-Q_e)}{2\,\hat{T}_d} \;, \qquad (3)$$

where Q_e describes the electronic losses of the target atoms as calculated from the Lindhard theory |10|, and $\hat{T}_d$ is the average displacement energy |11|. Finally in equation (1), T_d is the minimum threshold energy for displacement and T_m is the maximum energy a particle can transfer to a target atom.

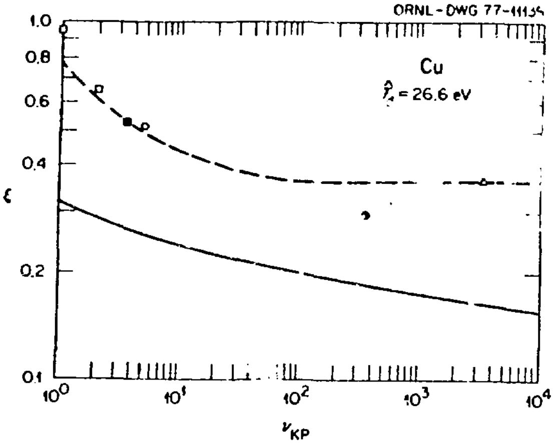

Fig. 1 Damage efficiency, ξ, as a function of cascade size for electrons (□) |12|, light ions (▣) |13|, thermal neutrons (○) |14|, fast neutrons (●) |14|, and self-ions (△) |13|. The dashed curve corresponds to a thermal spike model. The solid line includes thermal annealing process, using Eq. (4), for the cascade model shown in Fig. 2. In this case $\hat{T}_d = 1.4 T_d$ |11| and $f_{cp} = 0.28$ |48|.

Recent evaluations of low temperature data showed systematic deviations from the calculated $\nu_{KP}(T)$. These deviations can be described by inserting an efficiency factor, ξ into equation (1), which is given in Fig. 1 for Cu as a function of ν_{KP} for electron |12|, ion |13| and neutron |14| irradiation. It can be shown that these reduced efficiencies in low temperature experiments can be explained quantitatively by the self-annealing during cascade evolution according to a thermal spike model |15| (dashed line in Fig. 1).

On the other hand, simulation creep experiments are done at high temperatures, where the defects are mobile and thermal annealing processes after cascade formation will further reduce the number of defects which eventually will produce irradiation creep. This efficiency factor, which could be obtained from computer calculations on cascade annealing |16|, can be estimated in a simplified model by calculating the fraction of interstitials which succeed in escaping their own cascade. This escape probability is zero for a certain fraction, f_{cp}, of the defects produced (so-called close pairs), while the more distant interstitials have the probability $1 - r_i/r_p$ for escape, where r_i is the instability raduis for interstitials of the vacancy-rich cascade-core, and r_p is the average distance at which the interstitials are intitally stabilized (Fig. 2). Including the shrinkage of the cascade during the annealing, one obtains:

$$\xi = (1 - f_{cp})\left(1 - 2/3\,\frac{r_i}{r_p}\right)^{3/2} \qquad (4)$$

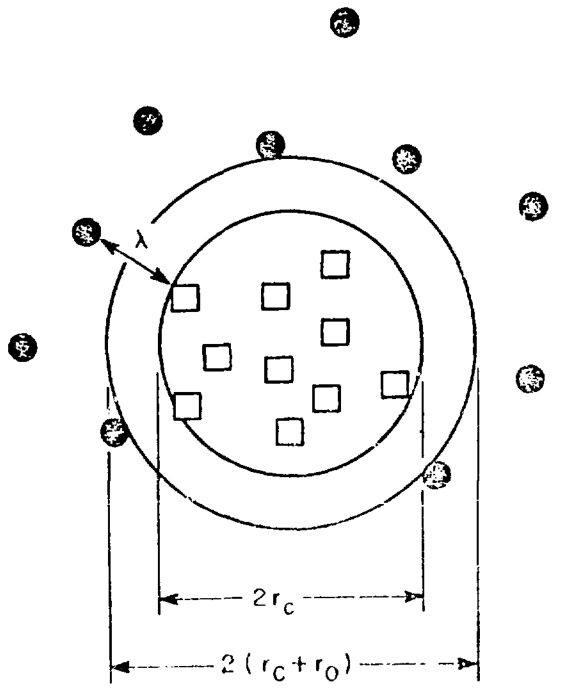

Fig. 2 Schematic view of the vacancy-rich core (radius r_c) of a cascade surrounded at an average distance λ by the interstitials. The instability radius r_i of the core for interstitials is $r_c + r_o$, where r_o is the instability radius of a single vacancy.

By inserting experimental values for the radii,* the solid line in Fig. 1 is obtained. Fig. 3 shows the displacement cross section, σ_d, as a function of the upper integration limit T_m for $\xi = 1$ (dashed line) and for the calculated high temperature efficiency given in Fig. 1.

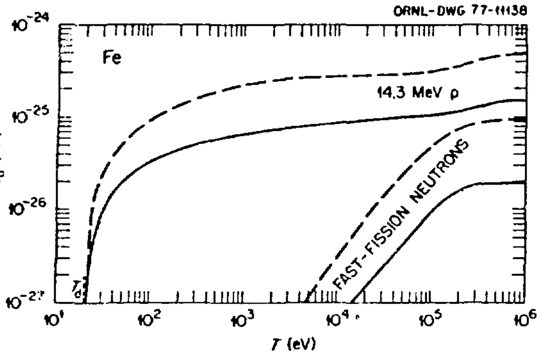

Fig. 3 Displacement cross section for 14.3 MeV protons and for a fast fission neutron spectrum calculated allowing no cascade annealing (- - -) and calculated using the damage efficiency shown by the solid line in Fig. 1 (——). The differential cross sections for the protons and the fast fission spectrum were taken from Ref. [49] and [50], respectively.

Three major differences between the damage structure obtained by charged particle versus neutron irradiation are derived from Fig. 3:

i. The cascade efficiency ξ reduces the number of escaping interstitials by a factor of about 3 for the protons and by 5 in the neutron case. This reduced dpa rate should be used, when comparing irradiation creep results to the theory; it gives the charged particle a somewhat higher relative efficiency for inducing creep compared to the neutrons.

ii. During the proton irradiation, most of the defects are produced in low energy cascades which are probably too small to form stable vacancy clusters and eventually loops. This may cause differences in the evolving microstructure, the influence of which is expected to be small in the SIPA model [22], but should be important if preferential loop nucleation is the dominant creep mechanism [23, 24].

iii. The small bumps at the end of the curves for protons come from recoil processes involving nuclear reactions. These make only small contribution to the total σ_d for the charged particles, but are appreciable for neutron damage even at much lower energies.

It is a shortcoming of all simulation techniques that the important consequences of nuclear reactions are almost missing. These are:

i. transmutation (alloying effects, phase instabilities)

ii. hydrogen and especially helium production (embrittlement, void nucleation).

Only the second point can be reasonably simulated, e.g. by homogeneously (and if possible, simultaneously) injecting helium by using an energy degrader or second accelerator.

---

* $r_i = r_c + r_o$, where r_c is the radius of the vacancy-rich core of the cascade [$r_c \approx 1.3 r_1 \cdot (\nu_{KP})^{1/3}$ [17-19], r_1 - interatomic distance], and r_o is the radius of the instability volume around a vacancy [$r_o \approx 2.4\ r_1$ [20]]; $r_p = r_c + \lambda$, where λ is the average distance between the interstitials and the core surface, [$\lambda \approx 3.8\ r_1$ [21]].

Energy Losses

So far the irradiation particles were treated as monoenergetic. Actually, charged particles suffer appreciable energy degradation when passing through matter. For the ions and energies of interest this is described by the nonrelativistic Bethe-Bloch formula |25|:

$$-\frac{dE}{d\kappa}\left[\frac{\mathrm{Mev}-\mathrm{m}^2}{\mathrm{kg}}\right] \approx 14.3\,\frac{Z_1^2\,M_1}{E[\mathrm{Mev}]}\cdot\frac{Z_2}{M_2}\;\ln\left(220\,\frac{E}{M_1 Z_2}\right). \qquad (5)$$

Integration of this equation up to the mass-thickness κ_o [kg/m^2], of the specimen can be accomplished by replacing E in the slowly varying ln-term by E(0), the incident particle energy. This gives the beam heating power, P_B, produced in the specimen by a given beam current I [μA]:

$$P_B[W] = \left(E(0) - E(\kappa_o)\right)\cdot\frac{I}{Z} = E(0)\cdot\left\{1-\left(1-\frac{2\kappa_o}{E(0)}\left(\frac{dE}{d\kappa}\right)_o\right)^{1/2}\right\}\cdot\frac{I}{Z_1} \qquad (6)$$

P_B is shown in Fig. 4 by the dashed curves for 14 MeV protons and 28 MeV alpha particles. This heat generation can place restrictions on the specimen thickness, beam current and/or minimum temperature of these experiments.

Since the displacement cross section is to a good approximation inversely proportional to the energy (Eq. (2)), the decrease in energy with penetration into the specimen leads to an increase in displacement rate across the sample thickness:

$$\frac{\sigma_d(\kappa)}{\sigma_d(0)} = \left(1-\frac{2\kappa}{E(0)}\cdot\left(\frac{\partial E}{\partial\kappa}\right)_o\right)^{-1/2} \qquad (7)$$

This is shown, also, in Fig. 4. The inhomogeneous displacement rate limits the sample thickness to avoid significant inhomogeneities in damage and, for a loaded specimen, stress. In foils the initial linearity in κ of equation (7) predicts fairly homogeneous damage in specimens of thickness up to about half the particle range, κ_R, when the specimens are intermittantly rotated. The particle range is approximated by:

$$\kappa_R\ [\mathrm{kg/m^2}] \approx 0.0105\,\frac{M_2}{M_1^{1/2}}\cdot\frac{E^{3/2}[\mathrm{MeV}]}{Z_1^2\,Z_2^{2/3}} \qquad (8)$$

In samples of nonuniform thickness, like wires or tubes, more complex analysis and manipulations would be necessary |26|.

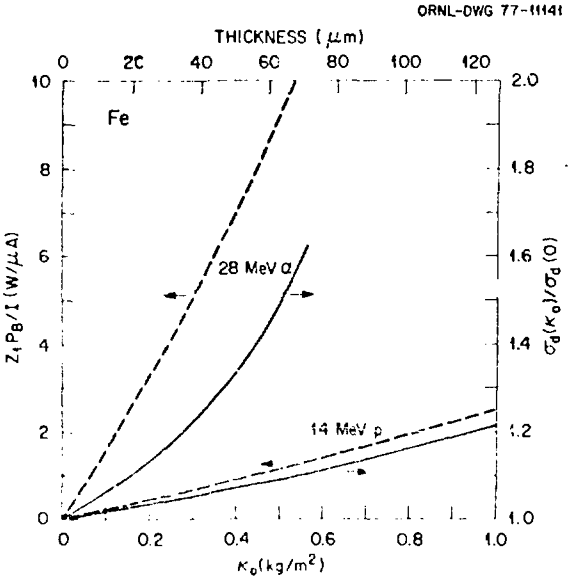

Fig. 4 Calculated electronic energy losses for 28 Mev alpha particles and 14 Mev protons given interms of beam heating power, P_B, and change in displacement cross section versus thickness or mass thickness, κ.

Sample Thickness Effects

From the above it is clear that thin specimens must be used in these experiments. With this limitation in thickness there arises a question of the validity of mechanical behavior where surfaces or surface effects may be important. The two major concerns are:

i. The interaction of dislocations and grain boundaries with the surface.

ii. The importance of surfaces in the chemical interaction with the environment, and the effect of this interaction on mechanical behavior.

It was shown recently |27| that stainless steel foils match the tensile behavior of bulk material at room temperature as long as the thickness exceeds about three grain diameters. Similar results on other materials may be found in Ref. |28|.

Only a very few thermal creep experiments on thin specimens have been reported. One of these studies again demonstrates the requirement that grain size be several times smaller than the minimum specimen dimension |29|. In recent experiments a Fe-Ni-Cr alloy showed at 695°C a pronounced effect of thickness |27|, which was attributed to surface oxidation. Annealed Ni foils |30| and 20% cold-worked 316 SS (this work) showed, at slightly lower temperatures, neither influence of thickness nor of a pure He environment on the thermal creep rate (Fig. 5).

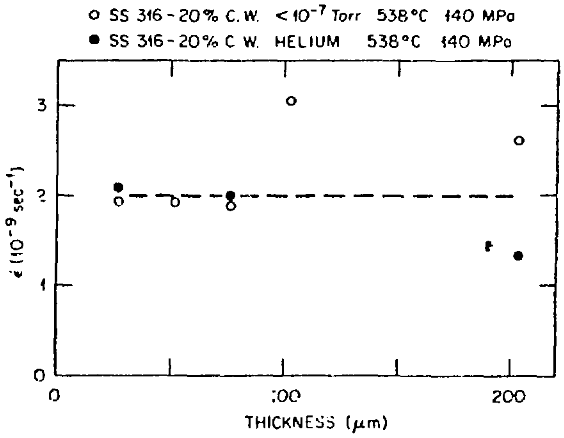
ORNL-DWG 77-11136

Fig.5 Thermal creep rate after about 170 hours as a function of thickness for 20%CW 316 SS in vacuum and in helium; specimen grain size is ≤ 10 μm.

Experimental Constraints

Besides the above mentioned constraints on sample thickness, there are further constraints on the experimental parameters which apply not only to simulation, but to all irradiation creep experiments:

i. The creep rate caused by the irradiation should be at least of the same order of magnitude as the thermal creep rate, to be separable. As the thermal creep rate strongly increases with temperature, while irradiation creep does not, this may set an upper limit to the irradiation temperature.

ii. The creep rate must exceed the observation limit of the apparatus. This is primarily determined by the available time and the overall temperature stability to avoid changes in specimen length by thermal expansions. For example, in stainless steel a change in specimen temperature of 1°C causes an elongation corresponding to a creep strain achieved after ∿ 50 hours in a fast reactor, when the sample is loaded at 138 MPa (20 ksi). Both these requirements and the desire to shorten the experiment time favor a high displacement rate, which naturally has an upper limit, set by the maximum beam current of the cyclotron and by the rate of specimen heat production, which for a given cooling rate will set a lower limit to the irradiation temperature.

Results and Current Experimental Efforts

Table 1.

[illegible]	MATERIAL, FORM	THICKNESS (µm)	PARTICLE, ENERGY (MeV) CURRENT DENSITY	STRESS (MPa)	TEMPERATURE	CALCULATED DISPLACEMENT RATE	CREEP RATE (sec⁻¹)	K^b (dpa⁻¹)	NUMBER OF SPECIMENS TESTED	REFERENCE	REMARKS
[illegible] F. [illegible] E. V. [illegible], Jr.	316 SS Solution-annealed^a foil	178	d^a 22.4	241-415	250-[illegible]	3 × 10⁻⁷	0.5 - 7.5 × 10⁻[illegible]	0.9 - 4.6	4	31	^a Degrader used
	304 SS Irradiated [illegible]	178	1.0 2.2	413	300		[illegible] × 10⁻[illegible]	0.2	1		^b Yielding occurred in 304 specimens
	316 SS 20% CW foil	178		130-186	[illegible]		0.3 - 1.[illegible] × 10⁻[illegible]	0.5 - 1.0	1		^c Stress exponent for 304 SS of 1 - 2 ^d Experiment terminated
[illegible] A. L. [illegible]	Ni CW foil	25	p^a 3.0 5.0	113	200	10⁻⁷	1.2 × 10⁻⁸	2.4	1	32	^a See also Ref. 33 ^b Limited T Control
[illegible]	Ni CW [illegible]	381	d^a 22.[illegible] 1.3-2.[illegible]	170-[illegible]	[illegible]	[illegible]	0.4 - [illegible]	[illegible] - 10.8	3	34	^a Stress exponent of 1.[illegible] - 2.0 observed
		381	[illegible]	170-345	[illegible]	[illegible] × 10⁻⁷	[illegible]3 - 1.2 × 10⁻[illegible]	[illegible] - 8.[illegible]	2		
[illegible]	Ni Annealed foil	25	p^a 4 [illegible]	[illegible]	[illegible]	[illegible] × 10⁻[illegible]	[illegible] - 2.9 × 10⁻[illegible]	[illegible].8 - [illegible]		35	^a Preoxidized specimens ^b Linear flux dependence observed ^c Decreasing strain rate with [illegible]
	[illegible] CW [illegible]	2[illegible]	p^a	[illegible]	[illegible]	[illegible] 1.8 × 10⁻[illegible]	0.[illegible] × 10⁻[illegible]	[illegible]		36	^a Preoxidized specimens ^b Linear flux dependence ^c Linear stress dependence (to 150 MPa) ^d Low temperature dependence
	[illegible] Annealed	2[illegible]	[illegible]	[illegible]	[illegible]	[illegible] × 10⁻[illegible]	[illegible] × 10⁻[illegible]	0.1			
	[illegible] Annealed	[illegible]	p^a	[illegible]	300-400	2 × 10⁻[illegible]	[illegible] × 10⁻[illegible]	[illegible]			
	Zircaloy 2 Annealed	[illegible]	5-10	[illegible]	300-[illegible]	2 × 10⁻[illegible]	[illegible]-1.[illegible] × 10⁻[illegible]	[illegible]		37	
[illegible]	[illegible] SS [illegible] CW wire	[illegible]	p^a [illegible].8	[illegible] MPa Shear Stress	500	[illegible] × 10⁻⁷	1.5 × 10⁻⁷ (Shear Strain Rate)	0.7^d	1	38	^a Torsion of wire specimen ^b Performed at [illegible]
[illegible]	316 SS [illegible]	40	d^a 16 [illegible]		[illegible]	[illegible] × 10⁻[illegible]	2.[illegible] × 10⁻[illegible]	[illegible]	1	39	^a Preliminary result
[illegible]		[illegible]	[illegible]						-	-	^a [illegible] complete
[illegible]			[illegible]						-	45	^a Limited, [illegible] results
[illegible]			[illegible]						-	46	^a Apparatus near completion
[illegible]	Ni	[illegible]	[illegible]	[illegible]	[illegible]		[illegible]		1	[illegible]	^a In liquid sodium ^b [illegible]

Irradiation creep measurements using light ion beams have been performed or will soon be performed at the laboratories listed in Table 1, which also lists the few experimental results to date. Data have been reported for stainless steels, nickel, zirconium and zircalloy-2. The first experiments at ANL in 1972 were performed at high stress on 304 and 316 SS [31]. Some preliminary results on Ni were reported by U. of Lowell, [32]; these experiments have recently been revived on zirconium-base alloys [33]. Hendrick, et. al. [34] performed a series of experiments on Ni. The most extensive results have been generated at AERE Harwell, in which Ni [35], 321 SS [36], Zr and Zircalloy [37] have been studied. Some very recent work at HEDL [38] and KFA Jülich [39] was done on 316 and 316L SS.

Several common features are observed in these experiments. First a low (1.0 to 2.0) stress exponent is observed. In the instances where the stress exponent exceeds unity, the applied stress values were fairly close to or exceeded the yield strength. Second, the Harwell results demonstrate and the NRL results are consistent with a linear flux dependence of the irradiation creep rate at displacement rates ∿ 10^{-7} to 10^{-6} dpa/sec. Also, a low temperature dependence in the creep rate of 321 SS is observed, under conditions where thermal creep contributions are small. One other feature has been noted in experiments on 321 SS [36]; there is a significant recoverable or anelastic strain component, having a linear stress dependence and a logarithmic time dependence.

Discussion

Insufficient information exists at this time to fully evaluate the potential of light ion irradiation as a simulation technique for neutron irradiation creep. However, the small temperature dependence and essentially linear stress dependence of the creep rate, $\dot{\varepsilon}$, induced by light ions allows us to use the quantity $\dot{\varepsilon}\mu/(K\sigma)$ [dpa^{-1}], where σ is the uniaxial stress, μ is the shear modulus and K is the displacement rate, to compare creep rates for stainless steels irradiated by light ions and by fast neutrons (Fig. 6).

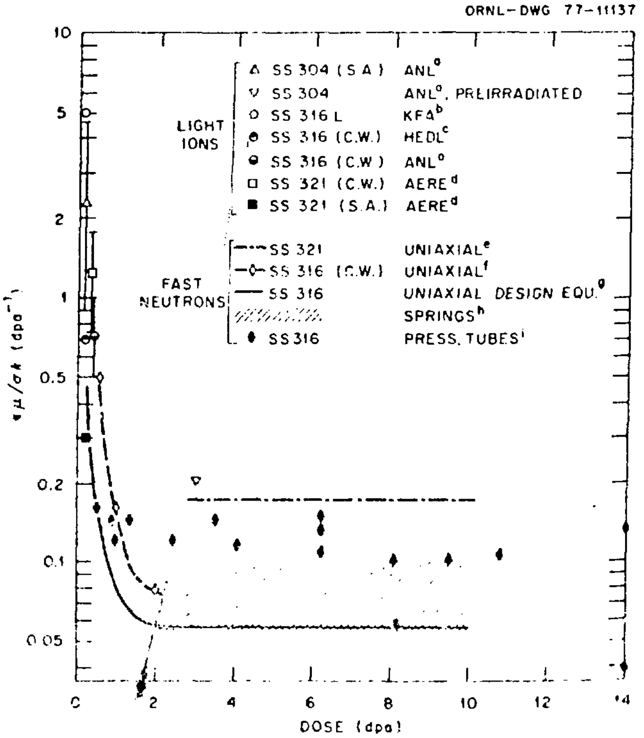

Fig. 6 Normalized irradiation creep rate, $\dot{\varepsilon}\mu/\sigma K$, versus dose for stainless steels irradiated with light ions and neutrons; a = Ref. [31], b = [illegible], c = [38], d = [36], e = [42], f = [40], g = [41], h = [43], i = [44].

It is seen, that at present simulation experiments extend only to doses below ~ 0.2 dpa, which have been inaccessible to in-reactor experiments due to their limited resolution. Fig. 6 is consistent with an extended transient region at low doses in which the creep rate decreases rapidly with dose. This transient behavior was observed in uniaxial stress experiments in the reactor |40| and is included in current design equations |41|. It should be pointed out that the only reported experiment on pre-irradiated material, 304 SS irradiated to ~ 3 dpa |31|, exhibits a value of $\dot{\varepsilon}\mu/\sigma K$ which is only about a factor of 2 above the uniaxial neutron results |40, 42-44|. This factor is quite consistent with our estimates regarding the higher efficiency factor for light ions.

The advantages of simulation over instrumented in-reactor experiments are ones of experimental versatility and economics. Instantaneous information is available in either case, but the strain resolution is higher for the simulation experiments due primarily to the better temperature control. This makes simulation especially useful for investigating transient effects or strain recovery as pointed out recently |42|. Further simulation work must extend to higher doses to clarify the importance of possible differences in the damage microstructure evolving from light ion versus neutron irradiations.

Another factor to be considered for simulation experiments using cyclotrons is the pulsed nature of the damage given by the high frequency (typically $\sim 10^7$ sec^{-1}) operation of the cyclotron and any lower frequencies which are sometimes used for beam scanning or rastering. On the other hand, dose rate effects are assumed to be small, since in simulation creep only slightly higher displacement rates than in fast reactors can be used, due to the problems of specimen cooling and the need for damage homogeneity, mentioned earlier.

From the standpoint of economics, it appears that simulation experiments have advantages over instrumented in-reactor experiments. While the operating costs of a creep rig in a fast reactor are estimated to be about half of the operation costs at a cyclotron, the slightly higher dpa-rates (factor 1-5), the one to two orders of magnitude higher strain resolution and a slightly higher duty factor of the equipment in a cyclotron experiment (due to the easier access and lower activity) should give the simulation an appreciable integrated advantage in time and cost. The costs for cyclotron use can be reduced drastically by using in-reactor pre-irradiated specimens. A subsequent simulation creep experiment allows instantaneous and accurate measurements of stress, temperature and displacement rate dependencies on materials at varying fluences. Possible transient effects associated with an undeveloped structure would be avoided.

Conclusions

In conclusion we may say that

i. Experiments using light ions to simulate irradiation creep are feasible and give self-consistent results.

ii. Irradiation creep by light ion irradiation shows the same phenomenological features as neutron results and the presently limited results are at least not inconsistant with neutron data.

iii. The limited thickness (25-200μm) poses no demonstrable problems in simulating bulk mechanical behavior at normal reactor temperatures.

iv. The high resolution and versatility makes simulation especially suited for the study of transient and strain recovery processes.

v. The use of pre-irradiation specimens in simulation experiments may be the most reasonable and most economic way to screen a large number of materials for their creep-resistance under irradiation.

Acknowledgement

The authors are indebted to the simulation creep groups at HEDL, NRL, PNL, U. of Lowell/MIT, AERE Harwell, CEN Saclay and GFK Karlsruhe for their helpful information on the present status of their experiments.

References

|1| E. N. Da C. Andrade, *Nature*, *156*, 113 (1945).

|2| W. F. Witzig, *J. Appl. Phys.*, *23*, 1263 (1952).

|3| M. R. Jeppson, R. L. Mather, A. Andrew, H. P. Yockey, *J. Appl. Phys.*, *26*. 365 (1955).

|4| J. J. Holmes, L. O. Petersen, *Phil. Mag.*, *16*, 845 (1967).

|5| J. Ponsoye, *Rad. Effects*. *8*, 13 (1971).

|6| I. Spitsyn, D. A. Troitskii, P. Ya. Glaznov, *Sov. Physics-Doklady*, *16*, 104 (1971).

|7| L. N. Bystrov, L. I. Ivanov, O. V. Martishin, *Rad. Effects*, *24*, 111 (1975).

|8| IAEA Specialists' Meeting, *Nucl. Eng. and Design*. *33*, 91 (1975)
D. G. Doran, J. R. Beeler, Jr., N. D. Duday, M. J. Fluss, USAEC Report HEDL-TME-73-76 (1973).

|9| G. H. Kinchin, R. S. Pease, *Rep. Prog. Phys.*, *18*, 1 (1955).

|10| J. Lindhard, V. Nielsen, M. Scharff, Kgl. Danske Videnskab Selskab, *Mat.-fys. Medd.*, *36*, No. 10 (1968).

|11| P. Lucasson in *Fundamental Aspects of Radiation Damage in Metals*, Gatlinburg 1975. CONF-751006-P1, p. 42.

|12| J. Wurm, Thesis, Report JÜL-581-FN (1969) (unpublished).

|13| K. L. Merkle in *Radiation Damage in Metals*, ASM-Seminar, Cincinnati (1975) p. 58.

|14| M. T. Robinson in *Radiation Damage in Metals*, ASM-Seminar, Cincinnati (1975) p. 1.

|15| G. Leibfried, *Bestrahlungseffekte in Festkorpern*, (1965) p. 257.

|16| J. G. Doran, J. O. Schiffgens in *Proc. Workshop on Correlation of Neutron and Charged Particle Damage*, Oak Ridge, 1976, CONF 760673, p.3.

|17| K. Merkle in *Radiation Damage in Reactor Materials*, Vienna 1969, Vol. 1, p. 159.

|18| L. E. Thomas, T. Schober, R. W. Balluffi, *Rad. Effects*, 1, 279 (1969).

|19| D. N. Seidman in *Radiation Damage in Metals*, ASM-Seminar, Cincinnati (1975) p. 28.

|20| G. Duesing, W. Sassin, H. Hemmerich, *Crystal Lattice Defects*, 1, 55 (1969).

|21| D. E. Becker, F. Dworschak, H. Wollenberger, *Rad. Effects*, 17, 25 (1973).

|22| P. T. Heald, M. V. Speight, *J. Nucl. Mater.*, 64, 139 (1977).

|23| R. V. Hesketh, *Phil. Mag.*, 7, 1417 (1962).

|24| F. A. Nichols in *Properties of Atomic Defects in Metals*, Argonne 1976, to be published in *J. Nucl. Mater*.

|25| R. S. Nelson, *The Observation of Atomic Collisions in Crystalline Solids*, J. Wiley and Sons, (1968) p. 32.

|26| D. L. Styris, R. H. Jones, O. K. Harling, G. L. Kulcinski, R. P. Marshall, Report Battelle BNWL-1961/UC-20 (1976). R. H. Jones, D. L. Styris in *Proc. of Second Topical Meeting on the Tech. of Controlled Nucl. Fusion*, Richland, 1976, p. 247.

|27| J. Auer, A. A. Sagües in *Radiation Effects and Tritium Technology for Fusion Reactors*, Gatlinburg 1975, CONF-750989, p. II-64.

|28| A. W. Thompson, *Scripta Met.* 8, 145 (1974).

|29| D. K. Matlock, W. D. Nix, *Met. Trans.* 5, 1401 (1974).

|30| R. J. McElroy, J. A. Hudson, R. J. Francis Report AERE-R 7998 (1976).

|31| S. D. Harkness, F. L. Yaggee, F. V. Nolfi, in *Proc. Conf. on Irradiation Embrittlement and Creep in Fuel Cladding and Core Components*, BNES, London, 1973, p. 259.

|32| P. L. Hendrick, A. L. Bement, Jr., O. K. Harling, *Nucl. Instruments and Methods*, 124, 389 (1975).

|33| J. T. DiMarzo, G. E. Lucas, M. Surprenant, G. J. Brown, presented at Amer. Nucl. Soc. meeting June, 1977.

|34| P. L. Hendrick, D. J. Michel, A. G. Pieper, R. E. Surratt, A. L. Bement, Jr., *Proc. Conf. Radiation Effects and Tritium Technology*, Gatlinburg, 1975, CONF-750989, p. II-84.

|35| R. J. McElroy, J. A. Hudson, R. S. Nelson, *op. cit.*, p. II-72.

|36| J. A. Hudson, R. S. Nelson, R. J. McElroy, *J. Nucl. Mater.*, 65, 279 (1977).

|37| R. J. McElroy, to be published.

|38| E. K. Opperman, J. L. Straalsund, to be published.

|39| C. Schwaiger, P. Jung, H.Ullmaier, to be published.

|40| E. R. Gilbert, D. C. Kaulitz, J. J. Holmes, T. T. Claudson, in Proc. Conf. on Irrad. Embrittlement and Creep in Fuel Cladding and Core Components, BNES, London, 1973, p. 239.

|41| General Electric Report, GEAP-13961, 1973.

|42| D. R. Harries, J. Nucl. Mater., 65, 157 (1977).

|43| D. Mosedale, G. W. Lewthwaite, Proc. Iron and Steel Inst. Conf. on Creep Strength in Steel and High Temperature Alloys, U. of Sheffield, 1972, pub. by The Metals Society, p. 169.

|44| E. R. Gilbert, J. F. Bates, J. Nucl. Mater., 65, 204 (1977).

|45| P. Jary, P. Blanchard, to be published.

|46| P. L. Hendrick, private communication.

|47| K. Herschbach, presented at Fruejahrstagung der Deutschen Physikalischen Gesellschaft Freudenstadt, 1976.

|48| A. Sosin, Phys. Rev. 126, 1698 (1962).

|49| D. A. Thompson, J. E. Robinson, R. S. Walker, A. M. Omar, A. B. Campbell, Radiation Effects and Tritium Technology for Fusion Reactors, Gatlinburg 1975, CONF-750989, p II-382.

|50| A. D. Warwick, J. Nucl. Mater., 55, 259 (1975).